RMetS

Royal Meteorological Society

Combining satellite data and models to estimate cloud radiative effect at the surface and in the atmosphere

Richard P. Allan*

Department of Meteorology/National Centre for Atmospheric Science, School of Physical and Mathematical Sciences, University of Reading, Reading, Berks RG6 6AL, UK

ABSTRACT: Satellite measurements and numerical forecast model reanalysis data are used to compute an updated estimate of the cloud radiative effect on the global multi-annual mean radiative energy budget of the atmosphere and surface. The cloud radiative cooling effect through reflection of short wave radiation dominates over the long wave heating effect, resulting in a net cooling of the climate system of -21 Wm^{-2}. The short wave radiative effect of cloud is primarily manifest as a reduction in the solar radiation absorbed at the surface of -53 Wm^{-2}. Clouds impact long wave radiation by heating the moist tropical atmosphere (up to around 40 Wm^{-2} for global annual means) while enhancing the radiative cooling of the atmosphere over other regions, in particular higher latitudes and sub-tropical marine stratocumulus regimes. While clouds act to cool the climate system during the daytime, the cloud greenhouse effect heats the climate system at night. The influence of cloud radiative effect on determining cloud feedbacks and changes in the water cycle are discussed. Copyright © 2011 Royal Meteorological Society

1. Introduction

Earth's radiative energy balance (solar radiative energy absorbed and terrestrial radiation emitted to space) determines current patterns of weather and climate, the complexity of which is illuminated by satellite observations of the evolving distribution and diversity of cloud structures. Representing clouds and the physical processes responsible for their formation and dissipation is vital in numerical weather and climate prediction, yet many approximations must be made in these detailed models of our atmosphere (e.g. Bony *et al*., 2006; Allan *et al*., 2007). Observations of cloud characteristics from satellite instruments and *in situ* or ground-based measurements are crucial for improving understanding of cloud processes and their impact on Earth's radiative energy balance (Sohn, 1999; Jensen *et al*., 2008; Su *et al*., 2010). The energy exchanges associated with cloud formation and precipitation are also a key component of the global water cycle, of importance for climate change (Trenberth, 2011).

In this paper, initially presented at a joint meeting of the Royal Meteorological Society and Institute of Physics on Clouds and Earth's Radiation Balance (Barber, 2011), the utility of combining weather forecast model output with satellite data in estimating the radiative effect of cloud is highlighted. Using a combination of models

and satellite data a simple question is addressed: how do clouds influence the radiative energy balance of the atmosphere and the surface.

As an example of the radiative impact of cloud, Figure 1 displays thermal infra-red and visible channel narrow-band images of the European region from the Spinning Enhanced Visible and Infra-Red Imager (SEVIRI) on board the Meteosat-9 satellite (Schmetz *et al*., 2002). In both images clouds appear bright: this denotes relatively low infra-red emission to space and relatively high reflection of visible sunlight to space. The hot, generally clear regions of northern Africa are also noticeable in both images since they are associated with substantial thermal emission to space (dark regions in the infra-red image) and high surface reflection from the desert surface (bright in the visible image).

The brightest clouds in the thermal image correspond with (1) a trailing cold front extending from the coast of Norway, across Scotland and to the west of Ireland, (2) a developing low pressure system to the west of Iceland, and, (3) a low pressure system in the Mediterranean centred on Sardinia. These are regions of ascending air with relatively high altitude, low temperature cloud tops which depress the thermal emission to space compared with surrounding regions. These features are also present in the visible image. However, many more cloud structures are also present. There is a prevalence of low altitude cloud over the oceans: this cloud contains large amounts of water droplets which are highly reflective (e.g. Stephens *et al*., 1978). The imagery captures the complex cellular structure of this cloud (e.g. Jensen *et al*., 2008) over the

∗ Correspondence to: R. P. Allan, Department of Meteorology, University of Reading, Whiteknights, Reading, Berks RG6 6AL, UK. E-mail: r.p.allan@reading.ac.uk
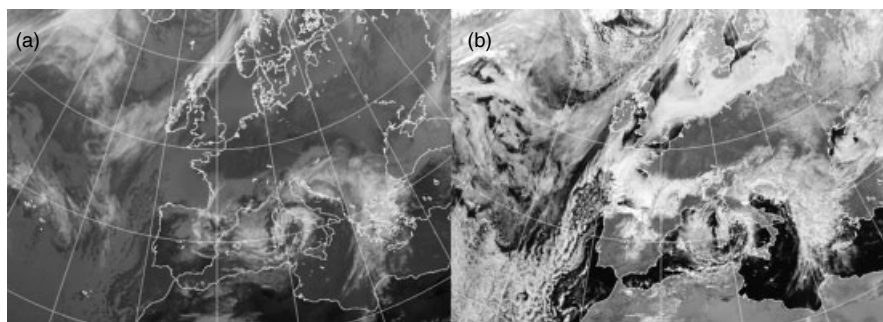
Figure 1. Satellite images from the SEVIRI geostationary satellite (a) 10.8 μm infra-red channel and (b) the 0.8 μm visible channel for 2 March 2011 at 1200 UTC. (© Copyright 2011, EUMETSAT/the Met Office).

region surrounding the Canary Islands. These cloud types are thought to contribute strongly toward uncertainty in climate projections (Bony *et al.*, 2006). While these clouds also strongly attenuate infra-red radiation, their impact on the thermal radiation escaping to space is modest since cloud-top temperatures are not dissimilar to the surface at night and so they do not contribute significantly to the strong natural greenhouse effect of the clear-sky atmosphere.

The altitude and optical thickness of cloud determines the overall radiative impact of cloud, a combination of the warming greenhouse effect and the surface-cooling solar shading effect. Yet, probably an even stronger influence does not relate to the cloud itself. The time of day and time of year dictate the incident solar radiation and, therefore, modulates the strength of the short wave reflection: clearly at night the solar influence of cloud is absent.

2. Cloud radiative forcing

To quantify the influence of cloud on Earth's radiative energy balance it is informative to consider separately the broadband long wavelength and short wavelength portions of the electromagnetic spectrum. To infer the influence of cloud on the radiation balance, the radiative fluxes over cloudy scenes may be compared with corresponding fluxes where the influence of cloud has been removed. This may be computed trivially in models by repeating the radiative transfer calculations and neglecting the effects of cloud but this method cannot be applied observationally. However, compositing radiative fluxes for clear-sky conditions and comparing with radiative fluxes for all scenes is one way to infer cloud radiative effect from satellite measurements, although this presents a difficulty in comparing model simulations with satellite estimates of cloud radiative forcing, CRF (e.g. Cess and Potter, 1987; Allan and Ringer, 2003; Erlick and Ramaswamy, 2003).

A further method is to combine simulations of clear-sky radiation with satellite measurements. An example of this is illustrated in Figure 2 which shows long wave and short wave cloud radiative effect over the Africa−Atlantic hemisphere. Although this does not constitute a radiative forcing of climate (Forster *et al.*, 2007), it is common practice to term the cloud radiative effect as a cloud

forcing (Ramanathan *et al.*, 1989). Here, long wave cloud radiative forcing (LWCF) is calculated as the difference between outgoing long wave radiation (OLR) and clear-sky OLR (OLRc):

$$LWCF = OLRc - OLR \qquad (1)$$

In the example in Figure 2, OLRc is provided by simulations made using the Met Office operational global Numerical Weather Prediction (NWP) model (Allan *et al.*, 2005) which uses the Edwards and Slingo (1996) radiative transfer scheme. The observationally-derived LWCF is presented in Figure 2(a) using OLR derived from radiances measured by the Geostationary Earth Radiation Budget (GERB) instrument (Harries *et al.*, 2005) onboard the Meteosat-9 satellite (preliminary version ARG-V006). The GERB instrument measures total and short wave broadband radiances (long wave radiances are calculated by subtraction) every 17 min at a sub-satellite nominal resolution of around 50 km. The radiances were converted to radiative fluxes using angular dependence models (Clerbaux *et al.*, 2008a, 2008b) that also rely on accurate information about the scene type (e.g. desert, ice cloud, etc), provided by SEVIRI also onboard Meteosat-9 (Schmetz *et al.*, 2002). The model-simulated LWCF is shown in Figure 2(b). Further details of the model and GERB data are provided elsewhere (Allan *et al.*, 2005, 2007; Harries *et al.*, 2005).

Similarly, the short wave cloud radiative forcing (SWCF) is defined as:

$$SWCF = RSWc - RSW \qquad (2)$$

where RSW is the reflected short wave radiation to space and clear-sky RSW (RSWc) is simulated by the NWP model. Figure 2(c) shows the GERB/model estimate of SWCF (multiplied by -1, since SWCF is usually negative, a cooling of the climate system): GERB RSW is adjusted by a factor, $f = S_m/S_g$, to account for a slight time offset of the model data (1200–1215 UTC) and the GERB data (1150–1205 UTC), where S is the incoming solar radiation at the top of the atmosphere for the model time (m) and the GERB data time (g). The model−SWCF is displayed in Figure 2(d).

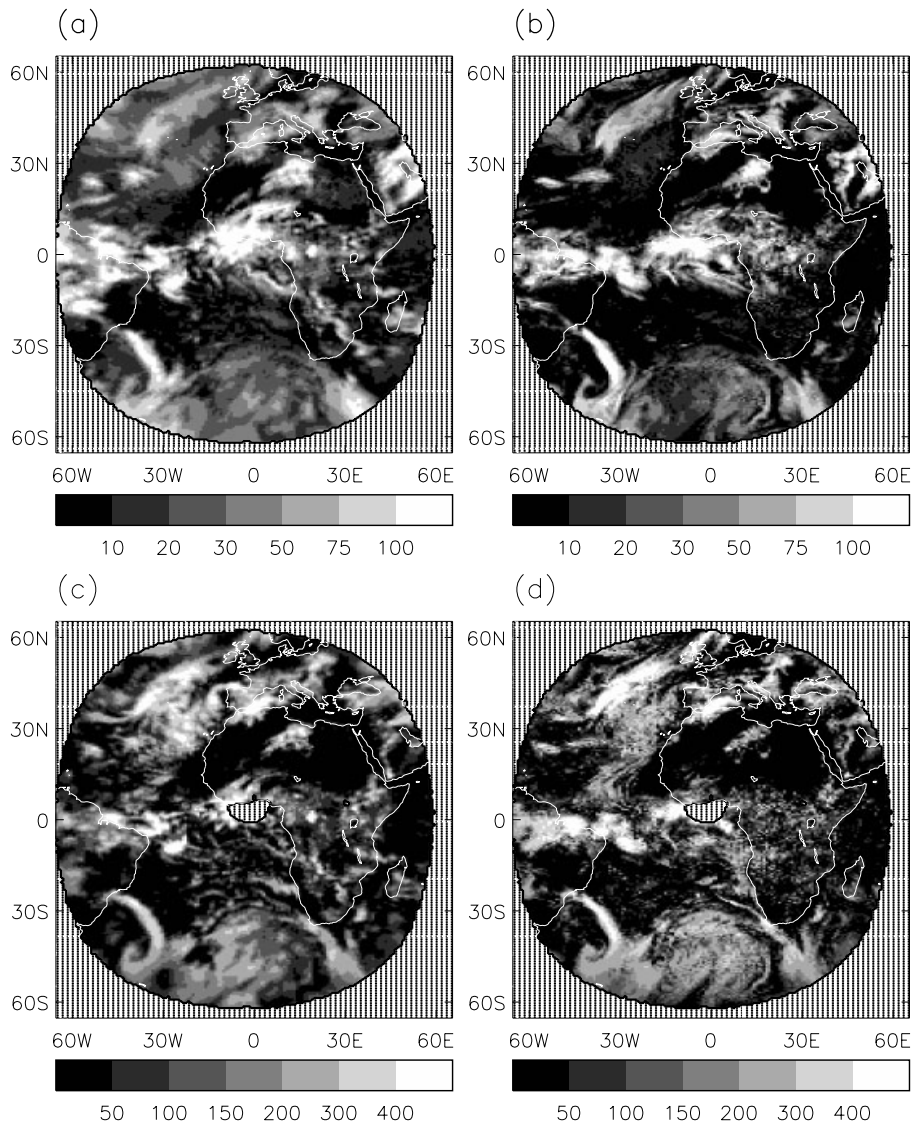The strongest LWCF (>100 Wm^{-2}) and SWCF (< -400 Wm^{-2}) occurs in the tropical rainy belt, a

Figure 2. Cloud radiative effect at 1200 UTC on 24 April 2011 calculated by combining GERB satellite data with NWP model clear-sky fluxes to generate (a) LWCF and (c) −SWCF and calculated using the model analysis field simulated (b) LWCF and (d) −SWCF. Missing GERB data are marked in both estimates by vertical lines.

region of extensive convective cloud associated with high short wave reflectivity (high albedo) and low cloud top emission from the high altitude, cold cloud-tops. Mid-latitude systems are also visible: an intense system over the Argentine basin (around 40 °W, 40 °S) and a trailing cold front over the North Atlantic. There is also extensive Canarian stratocumulus visible in Figure 2(c) (SWCF ∼ −300 Wm^{-2}) and extensive cloud over the Southern Ocean. It should be noted that the magnitude of SWCF is generally larger than the LWCF, one contributing factor being the proximity to local noon at which incident short wave radiation is strongest. This will be discussed further in Section 5.

While the model simulations capture the overall structure of CRF, there is a number of discrepancies which hint at the complexity in representing cloud systems, even for model analyses which are initialized from a previous model forecast using data assimilation to incorporate available observations. This is discussed elsewhere

(Allan *et al*., 2007) and is beyond the scope of the current study. Nevertheless the example in Figure 2 demonstrates the utility of combining models and satellite data in quantifying cloud radiative effect.

3. Global estimates of cloud radiative forcing

By flying well-calibrated broadband radiation instruments onboard low-Earth orbit satellites, high resolution, global estimates of the Earth's radiation budget may be built up over a period of days and months. As for the geostationary GERB data, measured radiances must be converted to radiative fluxes using angular dependence models (Loeb *et al*., 2007) valid for distinct scene types such as thick water cloud or cloud-free ocean. Using these data, composites of clear-sky and all-sky fluxes are constructed from which cloud radiative forcing may be estimated using Equations (1) and (2). The current set of Earth radiation budget instruments are from the Clouds
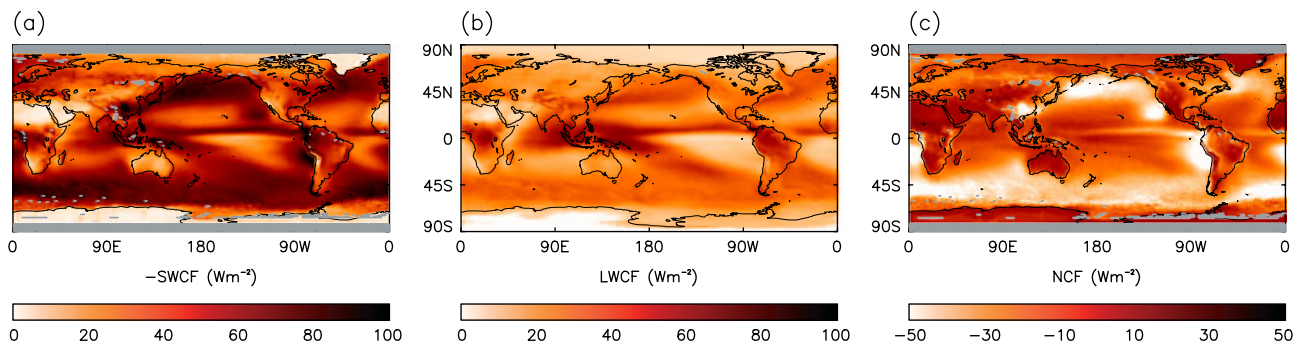
Figure 3. (a) Short wave (SW), (b) long wave (LW) and (c) Net cloud radiative effect relative to clear-sky conditions calculated from CERES satellite data for the period 2001–2007. Missing data is shaded grey. This figure is available in colour online at wileyonlinelibrary.com/journal/met

and the Earth's Radiant Energy System (CERES) sensors onboard the polar orbiting Terra and Aqua satellites (see Loeb *et al*., 2007). These have been providing global estimates of short wave, long wave and long wave window channel radiative fluxes since 2000.

Figure 3 shows the multi-annual mean top of atmosphere CRF from CERES on Terra (version 2.5Lite, a reduced set of products but with improved calibration compared to standard version 2 products) over the period 2001–2007. Clouds act to reduce the net incoming radiation through short wave reflection by up to about 100 Wm^{-2} (Figure 3(a)), in particular over the ocean storm-track regions, the tropical warm pool and Inter-Tropical Convergence Zone (ITCZ) and the extensive ocean stratocumulus decks off the coast of Peru, California and Namibia. The LWCF is strongest over the tropical warm pool, equatorial Africa and Columbia (up to 70 Wm^{-2}) where deep convective clouds reach the coldest points of the tropical tropopause. The net cloud radiative forcing:

$$NCF = LWCF - SWCF, \qquad (3)$$

is generally one of cooling, with the SWCF dominating the LWCF. This is most pronounced over the marine stratocumulus regimes and the mid-latitude storm-track regions with NCF more negative than -50 Wm^{-2}. Despite the substantial LWCF and SWCF over the tropical western Pacific and Indian ocean, their effects cancel to a large degree with NCF close to zero (Kiehl, 1994). NCF is also small over the clear regions of northern Africa, Australia and also over polar regions where temperature and cloud greenhouse effect is small and S is small. The overall global net cloud radiative effect is one of cooling as documented previously (Ramanathan *et al*., 1989).

4. Cloud radiative forcing of the atmosphere and at the surface

It has been established that, globally, the cooling effect of clouds through enhanced scattering of sunlight dominates over the enhanced cloud greenhouse heating effect when considered as annual averages. Are the heating and cooling effects acting at the surface or in the atmosphere? This is fundamental in linking the surface-atmosphere fluxes of energy, knowledge of which is important in understanding the coupling between the global energy and water cycles (Trenberth, 2011). There is a net radiative cooling of the atmosphere of around 100 Wm^{-2} and this is balanced by latent and sensible heat transfer from the surface to the atmosphere (e.g. Trenberth *et al*., 2009). Figure 4 shows estimates of the cloud radiative effect on the top of atmosphere, the atmosphere and the surface using 1° resolution global, gridded data from the NASA Surface Radiation Budget dataset (SRB version 3; Stackhouse *et al*., 2011). SRB combines radiative transfer models (Pinker and Laszlo, 1992; Fu *et al*., 1998) with satellite measurements of cloud properties from the International Satellite Cloud Climatology Project (ISCCP; Rossow and Schiffer, 1999) and reanalysis data (a fixed NWP model system incorporating data assimilation of available observations to produce a realistic three-dimensional simulation of weather systems; Bloom *et al*., 2005).

The SRB dataset is constrained at the top of the atmosphere by satellite measurements explaining the similarity in top of atmosphere cloud radiative effect in Figures 3 and 4(a)–(c). Differences in LWCF also relate to the contrasting methodologies of estimating OLRc: CERES OLRc is composited from clear-sky scenes which tend to contain lower than average monthly humidity compared to all-sky conditions from which the SRB calculates OLRc. Therefore CERES OLRc is higher than SRB OLRc in cloudy regions and from Equation (1) it may be explained why CERES LWCF is larger than SRB by around 10 Wm^{-2} over the Pacific ITCZ. There are also similar inconsistencies between measurements and simulations of RSWc due to systematic changes in aerosol and humidity between cloudy and clear scenes; using model simulations, Erlick and Ramaswamy (2003) found the definition of clear sky to impact the RSW by 8–10% over marine stratocumulus cloud. These issues are discussed further in previous studies (Cess and Potter, 1987; Allan and Ringer, 2003; Erlick and Ramaswamy, 2003; Sohn and Bennartz, 2008; John *et al*., 2011; Sohn *et al*., 2010).
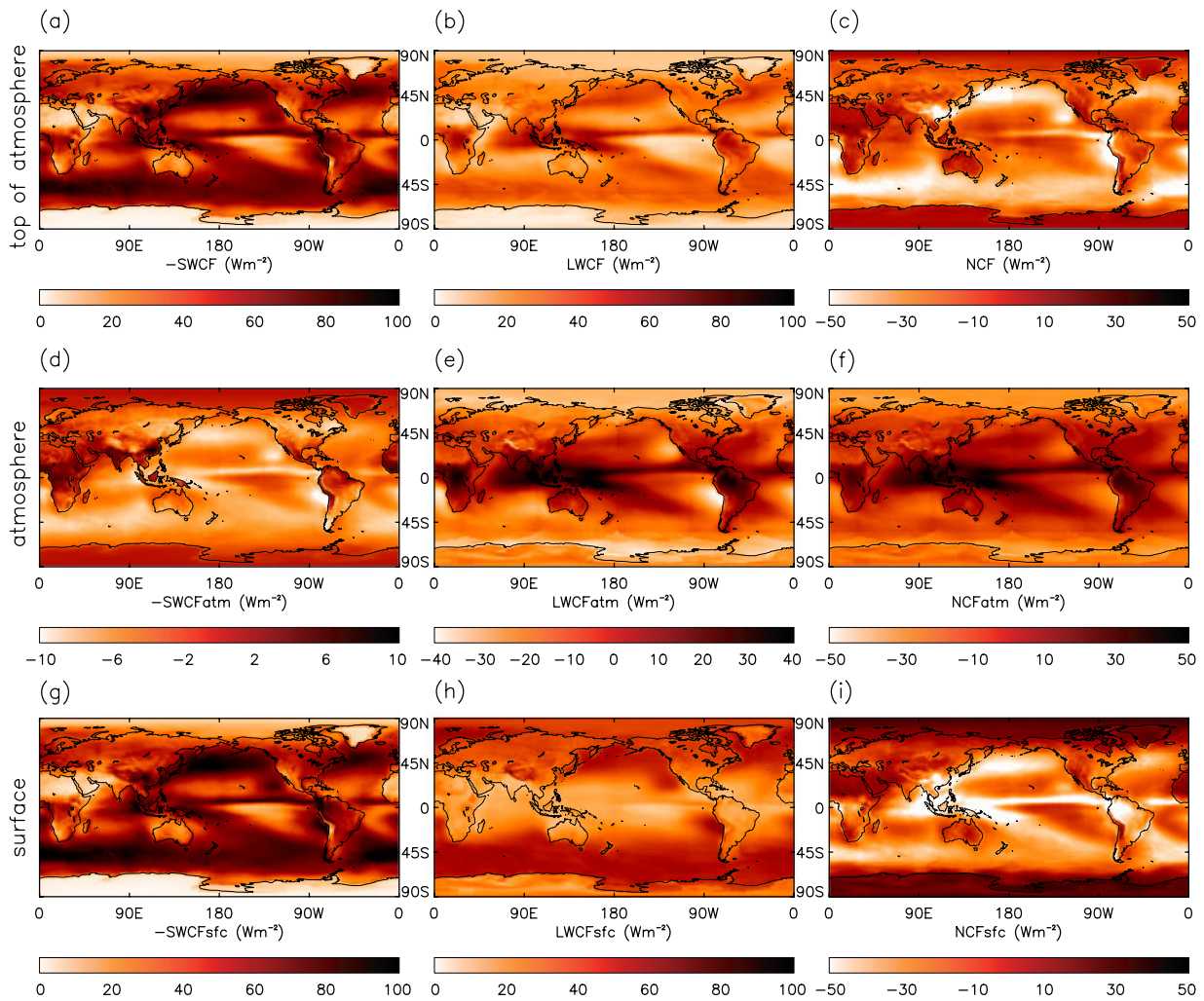
Figure 4. Negative short wave cloud forcing (−SWCF: a, d, g), long wave cloud forcing (LWCF: b, e, h) and net cloud forcing (NCF: c, f, i) calculated for the top of atmosphere (a–c) within the atmosphere (d–f) and at the surface (g–i) using the NASA Surface Radiation Budget product for the period 2001–2007. This figure is available in colour online at wileyonlinelibrary.com/journal/met

The advantage of the SRB methodology is that by combining reanalyses data with satellite retrievals and radiative transfer models, the entire month of clear-sky fluxes may be sampled, avoiding the more limited sampling of clear-sky fluxes using the CERES data alone and allowing direct comparison with climate model output. An additional advantage is that the SRB dataset allows an observational estimate of cloud radiative effect within the atmosphere (Figure 4(d)–(f)) and at the surface (Figure 4(g)–(i)). These are calculated as follows:

$$LWCFsfc = SDL - SDLc - SUL + SULc, \quad (4)$$

where SDL is the surface downwelling long wave radiation and SUL is the surface upwelling long wave radiation (c denotes clear-sky and sfc denotes surface). SUL is generally slightly larger than SULc (by 0.5 Wm^{-2} in the global annual mean) due to the additional long wave radiation emitted to the surface by clouds, a small proportion of which is reflected back by the surface, in particular for surfaces of low emissivity such as deserts where SUL can be up to 5 Wm^{-2} greater than SULc in the annual mean.

Similar to Equation (4), for the SWCF at the surface:

$$SWCFsfc = SDS - SDSc - SUS + SUSc, \quad (5)$$

where SDS is the surface downward short wave radiation and SUS is the surface upward (reflected) short wave (SUS = SDSα, where α is the surface reflection coefficient, or albedo and is spectrally dependent). Similarly for the atmosphere (atm),

$$LWCFatm = LWCF - LWCFsfc = OLRc$$
$$- OLR - SDL + SDLc + SUL - SULc, \quad (6)$$

and

$$SWCFatm = SWCF - SWCFsfc = RSWc$$
$$- RSW - SDS + SDSc + SUS - SUSc. \quad (7)$$

The NCFatm and NCFsfc are calculated as in Equation (3) for the atmosphere and the surface.

The negative SWCF is manifest primarily as a cooling of the surface with a residual heating effect applying in
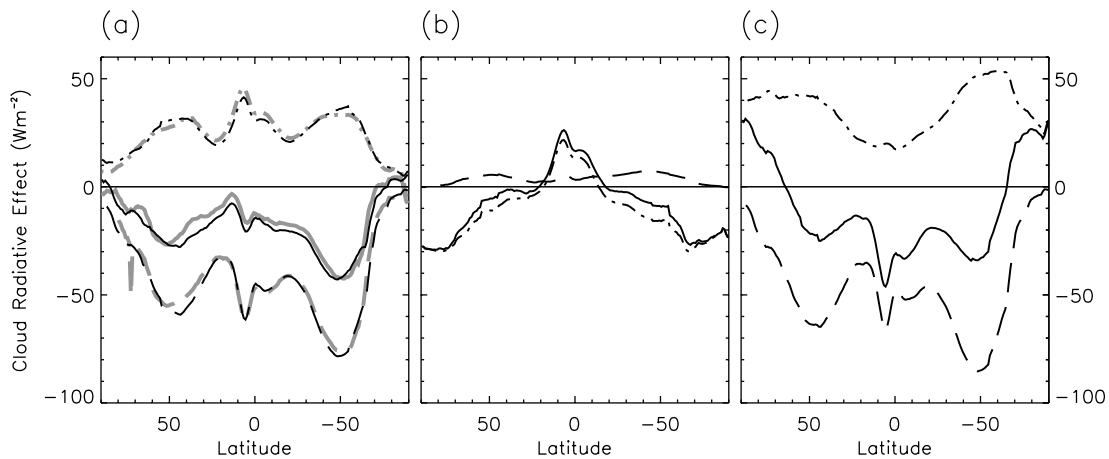
Figure 5. Zonal mean cloud radiative effect calculated for (a) the top of atmosphere, (b) within the atmosphere and (c) at the surface using the NASA Surface Radiation Budget product data for the period 2001–2007: — · — · LWCF; — — — SWCF; ———— NCF. Also shown in (a) are CERES observations: — · — · LWCF; — — — SWCF; ———— NCF.

the atmosphere that is less than 10 Wm^{-2} in magnitude. This heating effect relates to enhanced absorption of short wave radiation by the atmosphere above (primarily low-altitude) cloud decks rather than a direct absorption of short wave radiation by the cloud itself.

Conversely, much of the LWCF in the moist tropics is manifest as a heating of the atmosphere, especially for high altitude cirrus cloud; cloud emission to the surface is small here since much of the surface downward long wave radiation originates from emission by the moist, near-surface layers of the atmosphere (e.g. Prata, 1996). In higher latitudes, and also for sub tropical stratocumulus regimes, where clouds are generally lower altitude, the atmosphere is more transparent to long wave radiation and where temperature inversions are common, there is a cooling effect of clouds on the atmosphere and a strong heating effect at the surface (additional emission to the surface is larger than reduced emission to space), explaining the modest heating effect calculated and measured at the top of the atmosphere (e.g. Sohn, 1999).

The small NCF in the tropical warm pool (due to compensation between LWCF and SWCF) is manifest as a strong cloud long wave heating effect of the atmosphere and a short wave cooling effect at the surface. As such, the presence of deep convective cloud is acting to stabilize the atmospheric profile radiatively, modifying the radiative convective balance of the clear-sky atmosphere (e.g. Manabe and Wetherald, 1967). At higher latitudes, clouds enhance cooling of the atmosphere to the surface through long wave radiative transfer.

Figure 5 summarizes the zonal mean effect of cloud on the top of atmosphere, atmosphere and surface radiation balances, highlighting that clouds heat the atmosphere and cool the surface in the tropics while at high latitudes they enhance long wave emission from cloud base to the surface. Overall, NCF is negative at all but the highest latitudes due to the dominance of negative SWCF over positive LWCF for the annual mean.

Table I. Global multi-annual mean cloud radiative effect, 2001–2007.

Dataset	SWCF (Wm^{-2})	LWCF (Wm^{-2})	NCF (Wm^{-2})
CERES TOA	−47.4	28.2	−18.2
SRB TOA	−48.5	27.2	−21.3
SRB atmosphere	4.3	−5.5	−1.2
SRB surface	−52.8	32.7	−20.1

Global mean estimates of CRF are documented in Table I. Where CERES multi-annual mean data are missing, SRB values were inserted, thereby avoiding sampling differences (this altered the global mean values by less than 0.5 Wm^{-2}, primarily affecting SWCF). The global mean NCF is approximately −20 Wm^{-2} depending upon which dataset and method is used, and is comparable to estimates by Su *et al.* (2010). This cooling influence of clouds on the current climate system is primarily experienced at the surface; SWCF in the atmosphere is small and cloud long wave heating of the atmosphere in the tropics is counteracted by cloud radiative cooling of the atmosphere over higher latitudes (Figure 5).

5. The influence of time of day on cloud radiative forcing

As discussed in Section 1, the dominance of SWCF over LWCF in Figure 5 is only applicable for annual averages, or more specifically for annual diurnal averages and is not applicable for night time where SWCF becomes zero due to zero incoming solar radiation. This is illustrated in Figure 6 using the combination of GERB Edition 1 and NWP model data described in Section 2. All GERB short wave radiative fluxes are scaled by a factor of 0.976 to account for updated calibration information (J. Russell, personal communication 2011) and also by the factor S_m/S_g as discussed in Section 2. Zonal mean
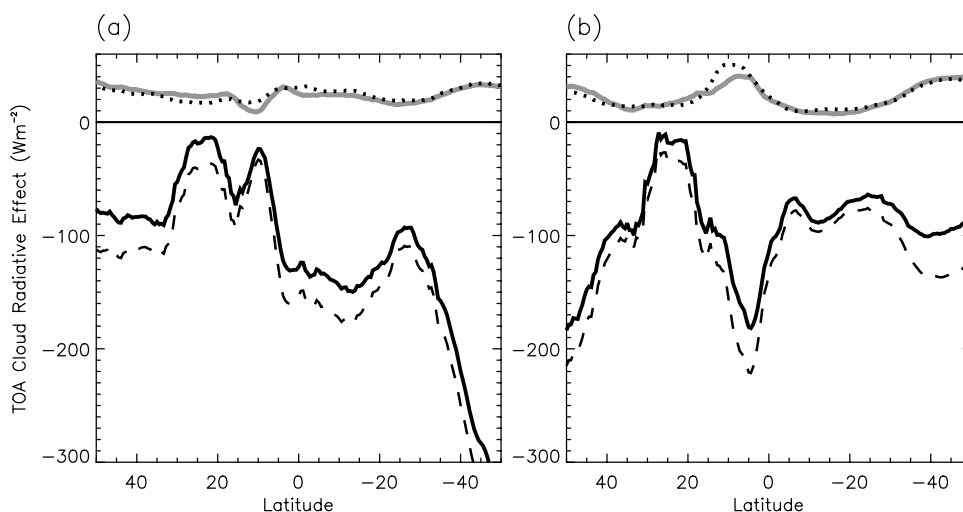
Figure 6. Zonal mean cloud radiative effect at 12 and 00 UTC for 30 °E to 30 °W estimated using GERB satellite data and NWP model clear-sky simulations for (a) November to January and (b) May to July over the period 2004–2007: ▬▬▬ NCF 12 UTC; − − · SWCF 12 UTC; ▬▬▬ LWCF 12 UTC; ······· NCF and LWCF 00 UTC.

CRF is calculated separately for 1200–1215 UTC and 0000–0015 UTC data over the period 2004–2007.

At 1200 UTC, the substantial incoming solar radiation leads to a large SWCF typically around −100 Wm^{-2} which dominates over the modest LWCF of around 10–40 Wm^{-2} (see also Figure 2). The SWCF is more negative than −300 Wm^{-2} at 45 °S in November to January (Figure 6(b)) highlighting the importance of season on SWCF at higher latitudes with extensive cloud in the Southern Ocean reflecting back to space a significant proportion of the considerable solar radiation incident during the southern hemisphere summer. However, at 0000 UTC (black, dotted line), SWCF is zero and the positive NCF is explained exclusively by the LWCF which is of similar magnitude and structure to the 1200 UTC values. Thus, the radiative effect of changes in cloud cover or properties is highly sensitive not only to cloud type (height, optical thickness, extent) but also to the time of year and time of day at which the changes in cloud properties take place. This is of importance in assessing cloud climate feedbacks which contribute substantially to uncertainty in climate prediction (Bony *et al.*, 2006).

6. Interannual changes in cloud radiative forcing

To assess cloud climate feedbacks, in addition to measuring cloud properties and assessing their representation by models, it is also informative to consider how cloud radiative effect changes with time (e.g. Wielicki *et al.*, 2002; Clement *et al.*, 2009; Dessler, 2010). The longest records of top of atmosphere radiation are from the CERES scanning instrument on the Terra satellite (2000–present) and from an earlier non-scanning radiation budget instrument (wide field of view, WFOV) onboard the Earth Radiation Budget Satellite (ERBS, 1985–2000), described in Wielicki *et al.* (2002). The WFOV instrument measures integrated radiative fluxes rather than scanning radiances

and so does not need to rely on angular dependence models but samples at a low spatial resolution (around 5° in latitude and longitude) and requires 72 days to completely sample the diurnal cycle of radiative fluxes necessary to build up diurnal-mean fluxes (Wielicki *et al.*, 2002; Wong *et al.*, 2006). The near-global region 60 °S to 60°N, the limit of the WFOV instrument, is considered in Figure 7 which shows net top of atmosphere radiation and NCF with the seasonal effects removed (de-seasonalized) for WFOV, CERES and also for a state-of-the-art reanalysis system, the European Centre for Medium-range Weather Forecasts (ECMWF) Interim reanalysis (ERA Interim; Dee *et al.*, 2011). ERA Interim is based upon the ECMWF integrated forecast system and uses four-dimensional data assimilation of observational data to provide a six-hourly three dimensional representation of the atmosphere since 1989 (further details in Dee *et al.*, 2011). The radiative transfer code used to simulate radiative fluxes is described by Morcrette *et al.* (2007).

Because the spatial and temporal resolution of the WFOV instrument is low it was not possible to construct clear-sky composites and to calculate NCF it was necessary to use simulations of clear-sky fluxes from ERA Interim. For consistency, and also to avoid the uneven spatial sampling of clear-sky regions, the same strategy in calculating NCF from CERES data is also adopted. The WFOV data provides flux estimates over 72 day averages which avoids aliasing in artefacts of orbital drift into the measurements of OLR and RSW (Wong *et al.*, 2006). In calculating NCF, clear-sky radiative flux estimates from ERA interim were interpolated onto this 72 day temporal grid before estimating NCF anomalies. Anomalies were computed with respect to the monthly averages over the entire respective data records. The WFOV anomalies were adjusted by the mean 1989–1990 WFOV anomaly minus the mean 1989–1990 ERA Interim anomaly such that mean anomalies over the period 1989–1990 agreed
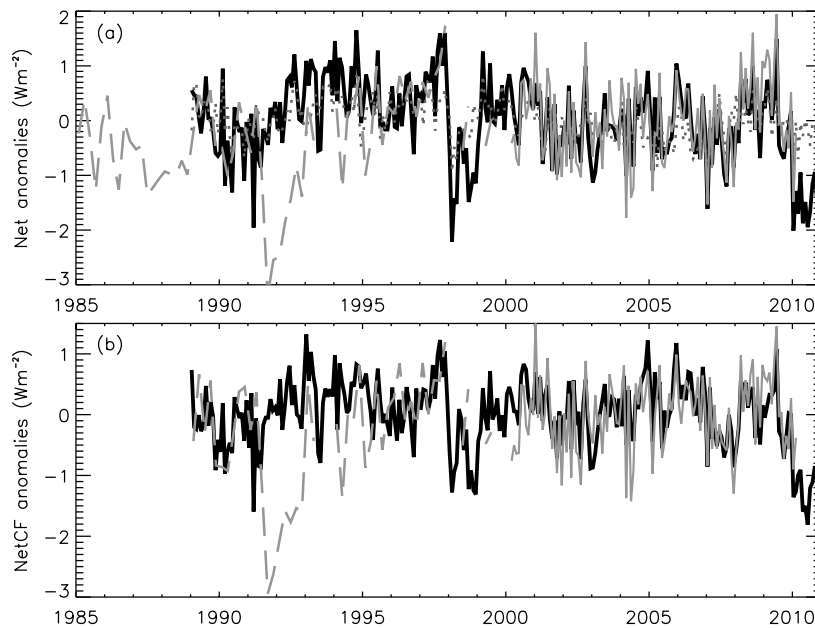
Figure 7. De-seasonalized monthly anomalies of (a) net radiation and (b) net cloud radiative forcing over the near-globe (60 °S to 60 °N) from ERA interim reanalysis, the ERBS wide field of view instrument and the CERES instrument on TERRA: — — ERBS WFOV; ——— CERES Ed2.5Lite; ▬▬ ERA Interim; ······ ERA Interim, clear-sky.

with ERA Interim. Also shown in Figure 7 are clear-sky net radiative flux anomalies simulated by ERA Interim.

Changes in net radiation appear relatively stable over the period 1985–2010, fluctuating by ± 1 Wm^{-2} with a few notable exceptions. The large negative anomalies in 1991–1993 in the WFOV data relate to the explosive eruption of Mt. Pinatubo in June 1991 which caused an increase in Earth's albedo due to the injection of reflective sulphate aerosols into the stratosphere, resulting in negative instantaneous radiative forcing of around 3 Wm^{-2} (e.g. Soden *et al.*, 2002). Since Pinatubo aerosols were not included in the ERA Interim simulations, the NCF calculated from WFOV-ERA Interim actually corresponds to a combination of cloud radiative effect and radiative forcing from Pinatubo over this period. Further inaccuracies in the simulation of clear-sky radiative fluxes due to the lack of representation of changes in aerosol radiative forcings will reduce the accuracy of NCF calculated in Figure 7. Nevertheless, with this caveat in mind, the comparison provides an interesting perspective on changes in NCF over recent decades.

For the remainder of the comparisons, there is remarkable agreement in changes in net radiative flux between CERES observations and ERA Interim (r = 0.83) and to a lesser extent WFOV and ERA Interim. Substantial negative anomalies in net radiative flux from ERA Interim are apparent in 1998 and 2010, both El Niño years, suggesting that the substantial re-organization of atmospheric and oceanic circulation systems act to remove energy from Earth during these periods. While a substantial proportion of the net flux change can be explained by the ERA Interim clear-sky fluxes in 1998, relating to an increase in OLRc due to substantial warming and drying of the subtropical descent regions (Chen *et al.*, 2002), there is an overall negative NCF simulated by ERA Interim

which appears to relate to a reorganization of clouds and associated SWCF. However, the negative anomalies in 2010 may be overestimated by ERA Interim compared to CERES estimates updated to December 2010 (N. Loeb, personal communication). Nevertheless, combining reanalyses datasets with satellite data potentially provides valuable information on Earth's energy flows and on how cloud radiative effects respond to and modify warming and cooling of the surface, critical in improving climate change projections.

7. Conclusions

Exploiting satellite measurements and combining them with NWP models initialized through assimilation of available observations enables the effect of clouds on the Earth's radiative energy balance at the surface and within the atmosphere to be quantified for the present day climate. Consistent with previous results (Ramanathan *et al.*, 1989; Su *et al.*, 2010), the cloud radiative cooling effect through reflection of short wave radiation is found to dominate over the long wave heating effect, resulting in a net cooling of the climate system of -21 Wm^{-2}. The short wave radiative effect of cloud is primarily manifest as a reduction in the solar radiation absorbed at the surface of -53 Wm^{-2} for the global multi-annual mean. The magnitude of this effect is strongly modulated by the incoming solar radiation and the dominance of cloud short wave cooling over long wave greenhouse trapping is maximum around local noon (Nowicki and Merchant, 2004) while the cloud long wave heating effect dominates at night. The long wave greenhouse effect of cloud measured at the top of the atmosphere is manifest primarily as a heating of the atmosphere in the moist

tropics, consistent with calculations by Sohn (1999). Over the marine stratocumulus regions and across higher latitudes the cloud-base emission to the surface becomes substantial and dominates over the reduced outgoing long wave radiation to space resulting in enhanced radiative cooling of the atmosphere and heating of the surface.

The cloud radiative influence on the exchange of radiative fluxes between the atmosphere and the surface are intimately linked with the water cycle through radiative-convective balance. While tropical, high-altitude clouds act to stabilize the atmospheric profile radiatively, clouds over polar regions tend to cool the atmosphere while heating the surface through enhanced atmospheric long wave radiative emission to the surface. In future work it would be informative to categorize these effects by cloud type further (e.g. Futyan *et al.*, 2005) and compare with climate model simulations. These analyses are vital in constraining cloud feedback processes further and in linking to future changes in the water cycle (Stephens, 2005; Bony *et al.*, 2006; John *et al.*, 2009). A particular challenge is the accurate quantification of surface radiative fluxes due to the sparse ground-based observing network (Roesch *et al.*, 2011) and also monitoring current changes in cloud radiative effect in satellite data, reanalyses and models (Wielicki *et al.*, 2002); combining meteorological reanalyses with satellite data and surface observations provide a vital methodology for meeting these challenges.

Acknowledgements

References

Allan RP, Ringer MA. 2003. Inconsistencies between satellite estimates of long wave cloud forcing and dynamical fields from reanalyses. *Geophysical Research Letters* **30**: 1491, DOI: 10.1029/2003GL017019.

Allan RP, Slingo A, Milton SF, Brooks ME. 2007. Evaluation of the Met Office global forecast model using Geostationary Earth Radiation Budget (GERB) data. *Quarterly Journal of the Royal Meteorological Society* **133**: 1993–2010.

Allan RP, Slingo A, Milton SF, Culverwell I. 2005. Exploitation of geostationary Earth radiation budget data using simulations from a numerical weather prediction model: methodology and data validation. *Journal of Geophysical Research* **110**: D14111, DOI: 10.1029/2004JD005698.

Barber CR. 2011. Clouds and Earth's radiation balance – observational evidence. *Weather* DOI: 10.1002/wea.825 (in press).

Bloom SJ, da Silva A, Dee D, Bosilovich M, Chern J-D, Pawson S, Schubert S, Sienkiewicz M, Stajner I, Wu M-L. 2005. Documentation and validation of the Goddard Earth Observing System Data Assimilation System–version 4. TM–2005–104606. NASA Washington, DC; 166 pp.

Bony SR, Colman R, Kattsov VM, Allan RP, Bretherton CS, Dufresne J-J, Hall A, Hallegatte S, Holland MM, Ingram W, Randall DA, Soden BJ, Tselioudis G, Webb MJ. 2006. How well do we understand and evaluate climate change feedback processes? *Journal of Climate* **19**: 3445–3482.

Cess RD, Potter GL. 1987. Exploratory studies of cloud radiative forcing with a general circulation model. *Tellus* **39**: 460–473.

Chen J, Carlson BE, Del Genio AD. 2002. Evidence for strengthening of the tropical general circulation in the 1990s. *Science* **295**: 838–841.

Clement AC, Burgman R, Norris JR. 2009. Observational and model evidence for positive low-level cloud feedback. *Science* **325**: 460–464.

Clerbaux N, Dewitte S, Bertrand C, Caprion D, De Paepe B, Gonzalez L, Ipe A, Russell JE. 2008a. Unfiltering of the Geostationary Earth Radiation Budget (GERB) data. Part II: long wave radiation. *Journal of Atmospheric and Oceanic Technology* **25**: 1106–1117.

Clerbaux N, Dewitte S, Bertrand C, Caprion D, De Paepe B, Gonzalez L, Ipe A, Russell JE, Brindley H. 2008b. Unfiltering of the Geostationary Earth Radiation Budget (GERB) data. Part I: short wave radiation. *Journal of Atmospheric and Oceanic Technology* **25**: 1087–1105.

Dee DP, Uppala SM, Simmons AJ, Berrisford P, Poli P, Kobayashi S, Andrae U, Balmaseda MA, Balsamo G, Bauer P, Bechtold P, Beljaars ACM, van de Berg L, Bidlot J, Bormann N, Delsol C, Dragani R, Fuentes M, Geer AJ, Haimberger L, Healy SB, Hersbach H, Hlm EV, Isaksen L, Kllberg P, Khler M, Matricardi M, McNally AP, Monge-Sanz BM, Morcrette JJ, Park BK, Peubey C, de Rosnay P, Tavolato C, Thpaut JN, Vitart F. 2011. The ERA-interim reanalysis: configuration and performance of the data assimilation system. *Quarterly Journal of the Royal Meteorological Society* **137**: 553–597.

Dessler AE. 2010. A determination of the cloud feedback from climate variations over the past decade. *Science* **330**: 1523–1527.

Edwards JM, Slingo A. 1996. Studies with a flexible new radiation code. I: choosing a configuration for a large-scale model. *Quarterly Journal of the Royal Meteorological Society* **122**: 689–719.

Erlick C, Ramaswamy V. 2003. Note on the definition of clear sky in calculations of short wave cloud forcing. *Journal of Geophysical Research* **108**: 4156, DOI: 10.1029/2002JD002990.

Forster P, Ramaswamy V, Artaxo P, Berntsen T, Betts R, Fahey DW, Haywood J, Lean DC, Lowe DC, Myhre G, Nganga J, Prinn R, Raga G, Schulz M, Van Dorland R. 2007. Changes in atmospheric constituents and in radiative forcing. In *Climate Change 2007: The Physical Science Basis. Contribution of Working Group I to the Fourth Assessment Report of the Intergovernmental Panel on Climate Change*, Solomon S, Qin D, Manning M, Chen Z, Marquis M, Avery KB, Tignor M, Miller HL (eds). Cambridge University Press: Cambridge, New York, NY; 129–234.

Fu Q, Yang P, Sun WB. 1998. An accurate parameterization of the infrared radiative properties of cirrus clouds for climate models. *Journal of Climate* **11**: 2223–2237.

Futyan JM, Russell JE, Harries JE. 2005. Determining cloud forcing by cloud type from geostationary satellite data. *Geophysical Research Letters* **32**: L08807, DOI: 10.1029/2004GL022275.

Harries JE, Russell JE, Hanafin JA, Brindley HE, Futyan J, Rufus J, Kellock S, Matthews G, Wrigley R, Last A, Mueller J, Mossavati R, Ashmall J, Sawyer E, Parker D, Caldwell M, Allan PM, Smith A, Bates MJ, Coan B, Stewart BC, Lepine DR, Cornwall LA, Corney DR, Ricketts MJ, Drummond D, Smart D, Cutler R, Dewitte S, Clerbaux N, Gonzalez L, Ipe A, Bertrand C, Joukoff A, Crommelynck D, Nelms N, Llewellyn-Jones DT, Butcher G, Smith GL, Szewczyk ZP, Mlynczak PE, Slingo A, Allan RP, Ringer MA. 2005. The geostationary earth radiation budget project. *Bulletin of the American Meteorological Society* **86**: 945–996.

Jensen MP, Vogelmann AM, Collins WD, Zhang GJ, Luke EP. 2008. Investigation of regional and seasonal variations in marine boundary layer cloud properties from MODIS observations. *Journal of Climate* **21**: 4955–4973.

John VO, Allan RP, Soden BJ. 2009. How robust are observed and simulated precipitation responses to tropical ocean warming? *Geophysical Research Letters* **36**: L14702, DOI: 10.1029/2009GL038276.

John VO, Holl G, Allan RP, Buehler SA, Parker DE, Soden BJ. 2011. Clear-sky biases in satellite infra-red estimates of upper tropospheric humidity and its trends. *Journal of Geophysical Research* **116**: D14108, DOI: 10.1029/2010JD015355.

Kiehl JT. 1994. On the observed near cancellation between long wave and short wave cloud forcing in tropical regions. *Journal of Climate* **7**: 559–565.

Loeb NG, Kato S, Loukachine K, Manalo-Smith N, Doelling DR. 2007. Angular distribution models for top-of-atmosphere radiative flux estimation from the Clouds and the Earth's Radiant Energy System instrument on the Terra Satellite. Part II: validation. *Journal of Atmospheric and Oceanic Technology* **24**: 564–584.

Manabe S, Wetherald RT. 1967. Thermal equilibrium of the atmosphere with a given distribution of relative humidity. *Journal of the Atmospheric Sciences* **24**: 241–259.

Morcrette J-J, Bechtold P, Beljaars A, Benedetti A, Bonet A, Doblas-Reyes F, Hague J, Hamrud M, Haseler J, Kaiser JW, Leutbecher M, Mozdzynski G, Razinger M, Salmond D, Serrar S, Suttie M, Tompkins A, Untch A, Weisheime A. 2007. *Recent Advances in Radiation Transfer Parameterizations*, ECMWF Tech. Memo 539. European Centre for Medium-range Weather Forecasts: Reading. http://www.ecmwf.int/publications/library/ecpublications/_pdf/tm/501-600/tm539_rev.pdf [accessed 28 June 2011]

Nowicki SMJ, Merchant CJ. 2004. Observations of diurnal and spatial variability of radiative forcing by equatorial deep convective clouds. *Journal of Geophysical Research* **109**: D11202.

Pinker R, Laszlo I. 1992. Modeling surface solar irradiance for satellite applications on a global scale. *Journal of Applied Meteorology* **31**: 194–211.

Prata AJ. 1996. A new long wave formula for estimating downwelling clear sky radiation at the surface. *Quarterly Journal of the Royal Meteorological Society* **122**: 1127–1151.

Ramanathan V, Cess RD, Harrison EF, Minnis P, Barkstrom BR, Ahmad E, Hartmann D. 1989. Cloud radiative forcing and climate: results from the Earth Radiation Budget Experiment. *Science* **243**: 57–63.

Roesch A, Wild M, Ohmura A, Dutton EG, Long CN, Zhang T. 2011. Assessment of BSRN radiation records for the computation of monthly means. *Atmospheric Measurement Technology* **4**: 339–354.

Rossow WB, Schiffer RA. 1999. Advances in understanding clouds from ISCCP. *Bulletin of the American Meteorological Society* **80**: 2261–2288.

Schmetz J, Pili P, Tjemkes S, Just D, Kerkmann J, Rota S, Ratier A. 2002. An introduction to Meteosat Second Generation (MSG). *Bulletin of the American Meteorological Society* **7**: 977–992.

Soden BJ, Wetherald RT, Stenchikov GL, Robock A. 2002. Global cooling after the eruption of Mount Pinatubo: a test of climate feedback by water vapor. *Science* **296**: 727–773.

Sohn B-J. 1999. Cloud-induced infrared radiative heating and its implications for the large-scale tropical circulation. *Journal of the Atmospheric Sciences* **56**: 2657–2672.

Sohn B-J, Bennartz R. 2008. Contribution of water vapor to observational estimates of long wave cloud radiative forcing. *Journal of Geophysical Research* **113**: D20107, DOI: 10.1029/2008JD010053.

Sohn BJ, Nakajima T, Satoh M, Jang H-S. 2010. Impact of different definitions of clear-sky flux on the determination of long wave cloud radiative forcing: NICAM simulation results. *Atmospheric Chemistry and Physics* **10**: 11641–11646.

Stackhouse PW Jr, Gupta SK, Cox SJ, Zhang T, Mikovitz JC, Hinkelman LM. 2011. 24.5-year SRB data set released. *GEWEX News* **21**: 10–12.

Stephens GL. 2005. Clouds feedbacks in the climate system: a critical review. *Journal of Climate* **18**: 237–273.

Stephens GL, Paltridge GW, Platt CMR. 1978. Radiation profiles in extended water clouds. III: observations. *Journal of the Atmospheric Sciences* **35**: 2133–2141.

Su W, Bodas-Salcedo A, Xu K-M, Charlock TP. 2010. Comparison of the tropical radiative flux and cloud radiative effect profiles in a climate model with Clouds and the Earth's Radiant Energy System (CERES) data. *Journal of Geophysical Research* **115**: D01105.

Trenberth KE, Fasullo JT, Kiehl J. 2009. Earth's Global Energy Budget. *Bull. Amer. Meteorol. Soc.* **90**: 311–323.

Trenberth KE. 2011. Changes in precipitation with climate change. *Climate Research* **47**: 123–138.

Wielicki BA, Wong T, Allan RP, Slingo A, Kiehl JT, Soden BJ, Gordon CT, Miller AJ, Yang S-K, Randall DA, Robertson F, Susskind J, Jacobowitz H. 2002. Evidence for large decadal variability in the tropical mean radiative energy budget. *Science* **295**: 841–844.

Wong T, Wielicki BA, Lee RB, Smith GL, Bush KA, Willis JK. 2006. Re examination of the observed decadal variability of earth radiation budget using altitude-corrected ERBE/ERBS nonscanner WFOV data. *Journal of Climate* **19**: 4028–4040.